Available online at www.sciencedirect.com
ScienceDirect
Journal of Nuclear Materials 362 (2007) 402–410
journal of nuclear materials
www.elsevier.com/locate/jnucmat

An improved model to evaluate the oxidation kinetics of uranium dioxide during dry storage

A. Poulesquen [a,*], L. Desgranges [b], C. Ferry [a]

[a] CEA-Saclay, Nuclear Energy Division, DPC/SECR, F-91191 Gif Sur Yvette cedex, France
[b] CEA-Cadarache, Nuclear Energy Division, DEC/SA3C, F-13108 Saint-Paul lez Durance, France

Abstract

During dry air storage, the oxidation of the spent fuel in case of cladding and container failure (accidental scenario) could be detrimental for further handling of the spent fuel rod and for the safety of the facilities. Recently, the phase transition sequence during the first step of parabolic oxidation kinetic has been challenged again and two well-distinguished intermediate products, U_4O_9 and U_3O_7 have been identified. Moreover, these observations have shown that the three phases (UO_2, U_4O_9 and U_3O_7) occur together. Starting from a previous model of grain oxidation based on finite difference approach, a new model, describing the parabolic oxidation kinetic, has been developed based on the oxygen atom diffusion. This model allows in one hand to take into account the occurrence of the three phases and in another hand to describe accurately the plateau behaviour. A comparison between the model and literature data obtained on non-irradiated powders has been carried out and shows that this model can describe the weight gain evolution as a function of time for different temperatures. The diffusion coefficients of oxygen in the two phases (U_4O_9 and U_3O_7) were obtained by fitting the model results to experimental data. The comparison with the values given in literature is quite good.

PACS: 28.41.Kw; 66.30.−h

1. Introduction

In dry air storage conditions, the oxidation of the spent fuel, due to an oxygen income into the fuel rod (accidental scenario in case of cladding and container failure), can entail some difficulties for the safety of the facility. Because of the residual power provided by the radioactive decay of the fission products, the spent fuel keeps a temperature significantly higher than the ambient. It is well known that the transformation of UO_2 to U_3O_8 implies an increase of volume of approximately 36%. This volume swelling may thus stress the cladding, which may split as a result. Moreover, the formation of U_3O_8 may increase the release of radionuclides from the waste package due to the increase of the specific area.

In the literature, it is commonly accepted that the oxidation of uranium dioxide at temperatures below 673 K can be described as a two steps' reaction: $UO_2 \rightarrow U_4O_9/U_3O_7 \rightarrow U_3O_8$ [1]. Generally, the U_4O_9 phase is preferentially encountered during the oxidation of spent fuel, but with an O/U atomic

* Corresponding author. Tel.: +33 1 69084957; fax: +33 1 69083242.
E-mail address: arnaud.poulesquen@cea.fr (A. Poulesquen).

0022-3115/$ - see front matter © 2007 Elsevier B.V. All rights reserved.
doi:10.1016/j.jnucmat.2007.01.084

ratio that may reach a higher value than the stoichiometry of the U_3O_7 phase [2]. On the other hand, the oxidation of unirradiated UO_2 powders involves U_3O_7 formation. Many authors have studied the oxidation kinetics of UO_2 powders on the basis of the thermal gravimetric analysis and X-ray diffraction data [1–11]. There is a general agreement between these studies. Indeed, their results show some typical isothermal gravimetric curve versus time for the oxidation of UO_2 powders. The weight gain curves at low temperature may be interpreted and modelled by two successive and limiting mechanisms [12,13]:

- the oxidation of UO_2 to U_3O_7 is controlled by the diffusion of oxygen through the more oxidized layer which is formed on the surface;
- the weight gain during the second stage appears in the form of a sigmoid and the formation of the swelling oxide U_3O_8 follows a nucleation-and-growth mechanism.

Concerning the nucleation and growth reaction mechanism, the consensus is less wide and a certain degree of uncertainty in estimating the rate and the activation energy of the process has been pointed out in a recent review [12].

The evolution of the O/U atomic ratio as a function of time and for several temperatures is reported in the literature [1,3,6,10,11,14]. Aronson et al. [1] have carried out some oxidation experiments on UO_2 powder in air for temperatures ranging between 456 K and 594 K. The authors report that for temperatures lower than 531 K, the O/U value of the oxidation plateau can reach 2.33 (U_3O_7 phase). Beyond 531 K, a sigmoidal second reaction step begins during which the formation of U_3O_8 phase ($O/U \approx 2.67$) occurs. Obviously, the duration of the plateau depends on the temperature [13]. These observations are also reported by Saito [10] who notices that below 548 K, the U_3O_8 phase is not reached. It is valuable to note that these tests were performed in a limited time and one should not exclude the recovery of the oxidation kinetic if the time of experiment is prolonged. Moreover, the UO_2 starting material the different authors used is not the same in terms of grain size distribution, initial stoichiometry, composition of air, which may induce slight discrepancies between the experimental results reported in literature.

Concerning the first step of oxidation ($UO_2 \rightarrow U_4O_9/U_3O_7$), up to now, the measured weight gain curves were modelled by either stationary or non-stationary laws. Stationary laws, known under the name of Jander are often used to interpret the transformation of UO_2 into U_4O_9/U_3O_7 [6,9,12]. Unfortunately, this law has no physical meaning, excepted at the beginning of reactions during which the product layer may be considered as a plane [14]. On the other hand, the stationary law, named Valensi or Ginstling–Brounshtein, has a better physical meaning and seems better to describe the parabolic oxidation kinetic [1,14]. Many authors [1,2,9] applied the non-stationary law (solution of the diffusion equation in spherical coordinates) to extrapolate their experimental curves. Generally, the use of these laws requires the knowledge of the chemical diffusion coefficient of oxygen in the UO_2 matrix D^O ($cm^2\ s^{-1}$) or the rate constant k ($cm^2\ s^{-1}$). The chemical diffusion coefficient of oxygen in the UO_2 matrix (D^O) have been studied extensively and the results have been reasonably consistent in the range 773–1673 K [1,15–18]. Reviews on the chemical diffusion coefficient of oxygen in the UO_2 matrix are available in the literature [17,18]. From these measurements and the kinetic data presented by various investigators, the activation energy may be obtained. According to authors, the activation energies vary in the range of 75–125 kJ mol^{-1} [1–3,6,10,9,15–17]. In a review, Mac Eachern [19] gathers all the data obtained on unirradiated and irradiated fuel and reported an average activation energy of 96 kJ mol^{-1}.

Recently, the phase transition sequence during the first step of parabolic oxidation kinetic has been challenged again and two well-distinguished intermediate products, U_4O_9 and U_3O_7 have been identified [14]. Moreover, these observations have shown that the three phases (UO_2, U_4O_9 and U_3O_7) occur together and it seems necessary to consider two simultaneous reactions: $UO_2 \rightarrow U_4O_9$ and $U_4O_9 \rightarrow U_3O_7$.

In order to take into account these new experimental observations and since non-stationary laws do not respect the sequence of phase observed in experiments (because they take into account only the two phases UO_2 and U_3O_7), the purpose of this paper is firstly to propose an improved model to describe the grain oxidation during the first parabolic reaction. Secondly, the model will be compared with the kinetic data given in the literature.

In a first part of the paper, the procedure of calculation of grain oxidation will be presented. Then, a comparison between the calculation results and

the literature data will be achieved in terms of weight gain curves and diffusion coefficients of oxygen. Finally, the use of this model to describe the oxidation of irradiated fuel fragments will be approached.

2. Modelling of UO_2 oxidation

A numerical model based on the finite differences method is proposed in order to improve the existing models and, especially, to take into account the new experimental observations concerning the structural evolution during the kinetics of oxidation (sequence of appearance of the phase $UO_2 \rightarrow U_4O_9 \rightarrow U_3O_7$ with coexistence of the three phases during the parabolic step).

The method consists in modelling two non-stationary superposed and interdependent oxidation fronts U_4O_9 and U_3O_7. It is supposed that the mechanisms of oxidation of UO_2 to U_4O_9 and U_4O_9 to U_3O_7 are similar. The model is based on the step by step resolution of the diffusion equation (Eq. (1)) in a sphere of radius R:

$$\frac{\partial C}{\partial t} = D^{O}\left(\frac{2}{R}\frac{\partial C}{\partial r} + \frac{\partial^2 C}{\partial r^2}\right), \tag{1}$$

D^{O} represents the chemical diffusion coefficient of oxygen in the UO_2 matrix ($cm^2\ s^{-1}$), dr and dt are the space and time steps, respectively.

When the concentration at the reactional interfaces reaches a sufficient value, the new phase is

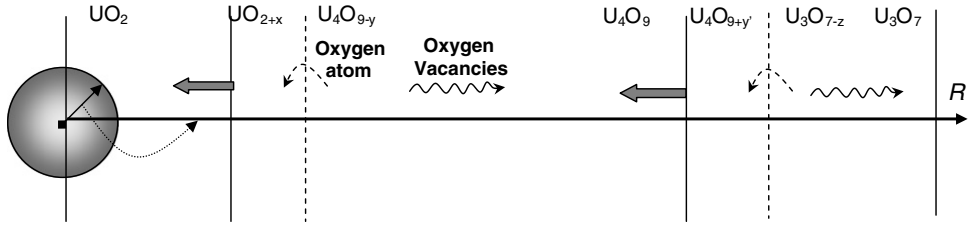

Fig. 1. Schematic representation of the oxidation model (v_O is the oxygen vacancies, R the grain radius and x, y, z correspond to hyper- and hypo-stoichiometric coefficients, respectively).

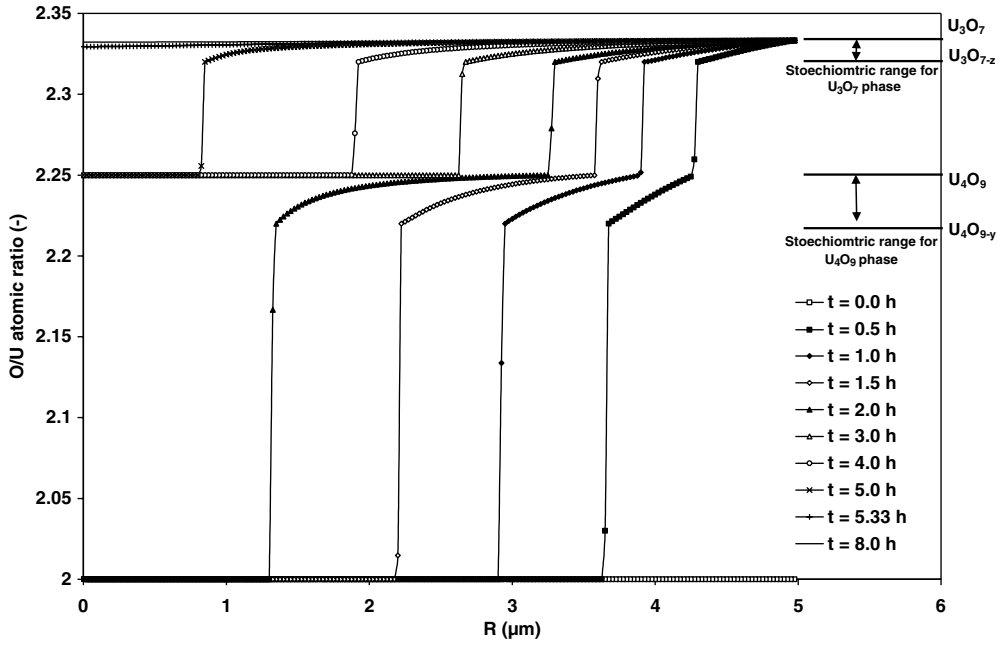

Fig. 2. Radial evolution of the O/U atomic ratio for a temperature of 523 K and a grain size of 5 µm ($D^{O}_{U_4O_9} = 6.1 \times 10^{-12}\ cm^2\ s^{-1}$ and $D^{O}_{U_3O_7} = 2.8 \times 10^{-12}\ cm^2\ s^{-1}$).

formed hypo-stoichiometric (U_3O_7 or U_4O_9). The driving of the diffusion is the gradient of stoichiometry in the two phases (Fig. 1). The values of the stoichiometry ranges have been fixed to [2.22–2.25] for the U_4O_9 phase and [2.32–2.33] for the U_3O_7 phase. These stoichiometry ranges were selected by taking into account the literature data and seem acceptable for modelling oxidation of unirradiated UO_2 grains. Numerical tests were carried out by modifying these stoichiometric domains and the results were quite similar. For the modelling of spent fuel oxidation, it will be necessary to take into account a more important variation of these ranges. Moreover, it is difficult to evaluate this parameter experimentally because of the presence of fission products and actinides dissolved in the matrix which modify the value of the O/U atomic ratio reached at the oxidation plateau.

The calculation starts with a first layer of U_4O_9 on the surface. The parameters of the model are the stoichiometries at the two phases U_4O_9 and U_3O_7 interfaces (which are fixed in our model) and the chemical diffusion coefficient of oxygen in these two same phases $D^{O}_{U_4O_9}$ and $D^{O}_{U_3O_7}$.

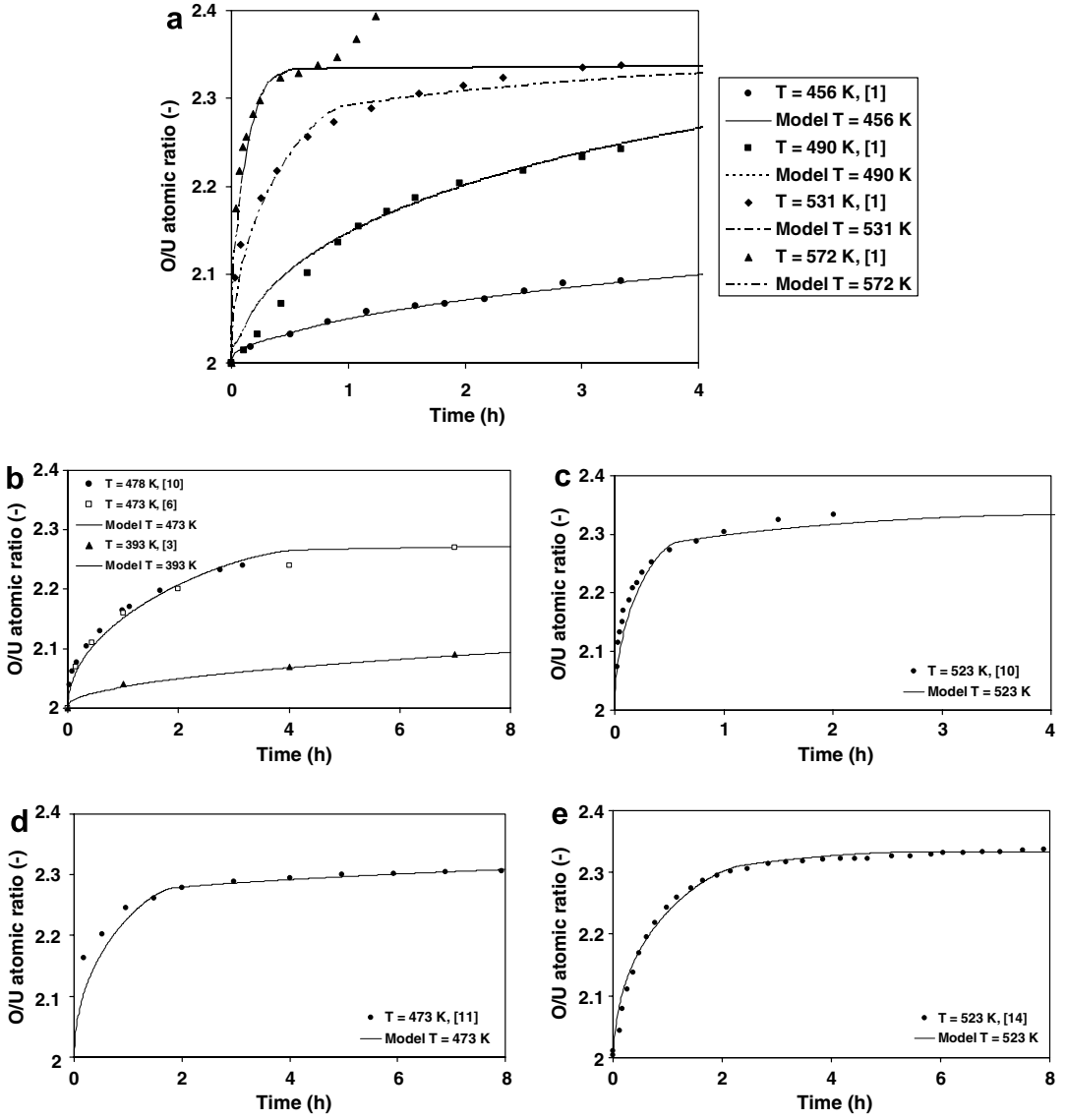

Fig. 3. Comparison between the calculation and literature data: (a)_[1], (b)_[6, 10, 3], (c)_[10], (d)_[11], (e)_[14]. *Note:* in Fig 3(a), for $T = 592$ K, the increase of weight gain is due to the apparition of U_3O_8 phase which is not taken into account in our model.

The evolution of the radial composition profile as calculated using our model for several oxidation times (temperature of 523 K and a grain size of 5 μm) is presented in Fig. 2. At the beginning of oxidation (oxidation time lower than 3 h), the occurrence of the three phases (UO_2, U_4O_9 and U_3O_7) in the grain is noticed. The reactional interfaces (or oxidation front), represented by an abrupt evolution of the O/U atomic ratio for the two transitions UO_2 to U_4O_9 and U_4O_9 to U_3O_7, progresses radially in the grain with oxidation time. Then for an oxidation time greater than 5 h, the grain is entirely in the stoichiometric range of U_3O_7 phase and consequently a classical non-stationary diffusion profile is obtained.

To compare the model with the literature data, the parameterization has been done exclusively on the diffusion coefficients of oxygen in the two phases ($D^{O}_{U_4O_9}$ and $D^{O}_{U_3O_7}$).

3. Comparison with literature data

3.1. Comparison to literature weight gain curves

A comparison between the grain model which has been described in the previous paragraph and the literature kinetic data is given in Fig. 3(a)–(e). The weight gain curves can be correctly modelled by fitting the values of diffusion coefficients of oxygen in U_4O_9 and U_3O_7 phases, whatever the temperatures ranging 393 and 572 K. Calculations were carried out for a grain radius of 5 μm (approximately the typical grain size in as-fabricated UO_2 fuel) and for a space discretization to 200 layers. It should be noted that the model begins at a O/U atomic ratio of 2.00, which is seldom the case in the experiments. This can explain the slight discrepancy between the model and the experiment at the beginning of the oxidation. The differences between the model results and experimental data can be also explained by the size of grains chosen for the calculations. Indeed, in experimental conditions, there is certainly a distribution of grain size which was not tested by the current model. This point will be approached later on.

In addition, on the Fig. 3(a), for $T = 572$ K, the comparison with the experimental data is less good. Basically, at this temperature, as we previously saw, the U_3O_8 phase certainly appears during the oxidation (Fig. 3(a)). On the plateau of oxidation, the coexistence of U_3O_7 and U_3O_8 phases surely takes place which is not taken into account by the model limited to $UO_2/U_4O_9/U_3O_7$ phases.

Thus, it appears that the experimental weight gain curves can be described with this oxidation model by an adjustment of the diffusion coefficients of oxygen in U_4O_9 and U_3O_7 phases and for temperatures lower than 523–533 K. The diffusion coefficients of oxygen in the U_4O_9 and U_3O_7 phases used in our model to fit the literature data are given in Table 1.

Table 1
Diffusion coefficient values of oxygen in U_4O_9 and U_3O_7 phases used in the model to fit experimental weight gain curves of the literature

References	T (K)	$D^{O}_{U_4O_9}$ ($cm^2\ s^{-1}$)	$D^{O}_{U_3O_7}$ ($cm^2\ s^{-1}$)
[3]	393	5.00×10^{-13}	5.00×10^{-16}
[1]	456	8.80×10^{-13}	4.00×10^{-14}
[11]	473	2.00×10^{-11}	1.50×10^{-12}
[6]	473	9.20×10^{-12}	2.00×10^{-13}
[10]	478	9.20×10^{-12}	2.00×10^{-13}
[1]	490	4.50×10^{-12}	2.00×10^{-12}
[14]	523	1.35×10^{-11}	5.70×10^{-12}
[10]	523	6.50×10^{-11}	8.00×10^{-12}
[1]	531	3.70×10^{-11}	6.00×10^{-12}
[1]	572	9.00×10^{-11}	5.50×10^{-11}

3.2. Comparison to diffusion coefficients of oxygen and associated activation energies

A comparison between the diffusion coefficients of oxygen in the two phases and the Arrhenius laws issued from the literature [1,12,16–18] is presented in Fig. 4. The values obtained with the model for the diffusion coefficient in the U_4O_9 phase (named Fit 1 in Fig. 4) are higher than the literature data. On the other hand, those relative to U_3O_7 (named Fit 2 in Fig. 4) are located in the panel of curves. Nevertheless, it is important to keep in mind that the mathematical expressions given in the literature have been deduced from measurements performed at temperatures greater than 773 K. Consequently, the comparison with our modelling results has been performed by extrapolating these mathematical expressions. It is also noticed that the diffusion coefficients of oxygen in U_4O_9 and U_3O_7 phases intersect around 573 K. This value of temperature is interesting since Dehaudt [20] in its review reported that for $T > 623$ K, U_3O_8 oxide appears alone in the case of powders of huge specific surface area. When the specific surface area is smaller, the temperature,

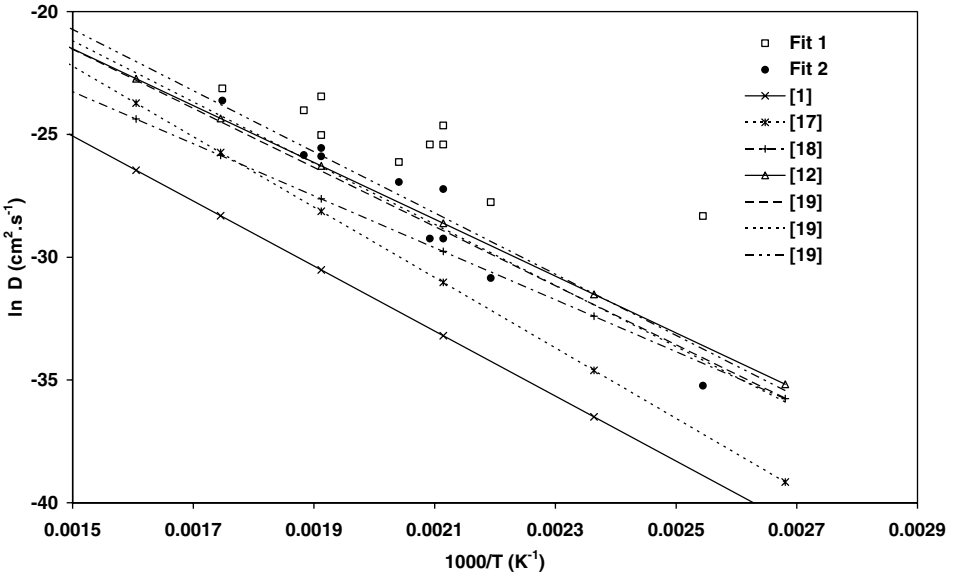

Fig. 4. Diffusion coefficients of oxygen obtained by fitting the oxidation model to literature data. Fit 1 and Fit 2 correspond to the diffusion coefficient of oxygen in U_4O_9 and U_3O_7 phases respectively.

Table 2
Activation energy and pre-exponential term issued from the fitting parameters $D^{O}_{U_4O_9}$ and $D^{O}_{U_3O_7}$

Phase	E_a (kJ mol^{-1})	D_0 (cm^2 s^{-1})
U_4O_9	57	1.36×10^{-5}
U_3O_7	123	1.16×10^{1}

beyond which only U_3O_8 appears, decreases to 523 K.

From Table 1 and by using the Arrhenius law for the diffusion coefficients, (Eq. (2)), the values of activation energy and the pre-exponential term (cm^2 s^{-1}) might be obtained, (Table 2).

$$D = D_0 \exp\left(-\frac{E_a}{RT}\right). \quad (2)$$

These activation energy values are in agreement with the literature data since a value of 90 kJ mol^{-1}

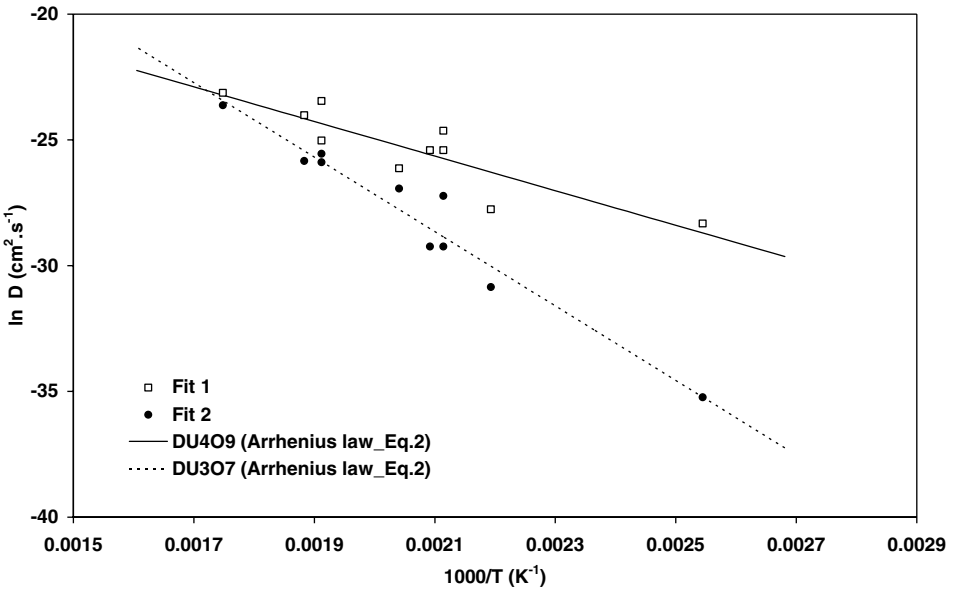

Fig. 5. Oxygen diffusion coefficient values in U_4O_9 and U_3O_7 phases.

is obtained on average [12]. Lastly, the computed values from parameters of Table 2 and the data resulting from the adjustment (Table 1) are represented in Fig. 5. The intersection of the curves occurs around 573 K ($1000/T = 1.748\ K^{-1}$).

4. Discussion

The modelling of the oxidation kinetics of a UO_2 grain by taking into account the U_4O_9 and U_3O_7 phases not only makes it possible not only to improve the quality of modelling, but also to better understand the phenomenology of oxidation, and finally to simulate the oxidation kinetics of irradiated fuel. With this new approach which allows describing the grain oxidation phenomenon by choosing suitable chemical diffusion coefficients of oxygen for the two phases, it is possible on the one hand, to describe the kinetics (fast) in the first moments of oxidation and on the other hand, to describe the evolution of the oxidation plateau (Fig. 6). The location of the plateau (value lower

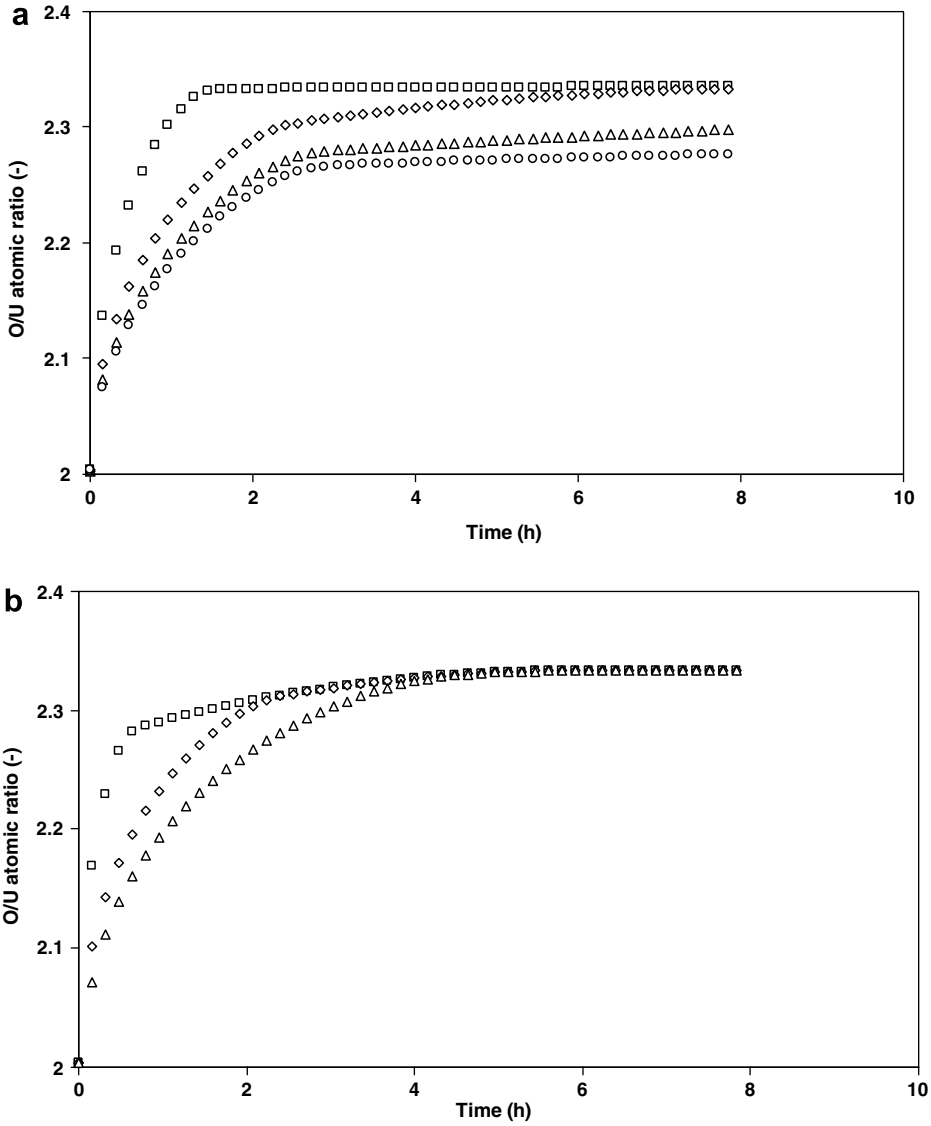

Fig. 6. (a) Oxidation kinetics for various diffusion coefficients of oxygen in the U_3O_7 phase. $D^{O}_{U_4O_9} = 1.35 \times 10^{-11} cm^2 s^{-1}$ and (□) $D^{O}_{U_3O_7} = 2.0 \times 10^{-11} cm^2 s^{-1}$; (◇) $D^{O}_{U_3O_7} = 4.0 \times 10^{-12} cm^2 s^{-1}$; (△) $D^{O}_{U_3O_7} = 1.0 \times 10^{-12} cm^2 s^{-1}$; (○) $D^{O}_{U_3O_7} = 3.0 \times 10^{-13} cm^2 s^{-1}$; (b) Oxidation kinetics for various diffusion coefficients of oxygen in the U_4O_9 phase. $D^{O}_{U_3O_7} = 5.7 \times 10^{-12} cm^2 s^{-1}$ and (□) $D^{O}_{U_4O_9} = 6.0 \times 10^{-11} cm^2 s^{-1}$; (◇) $D^{O}_{U_4O_9} = 1.35 \times 10^{-11} cm^2 s^{-1}$; (△) $D^{O}_{U_4O_9} = 5.7 \times 10^{-12} cm^2 s^{-1}$.

than O/U atomic ratio = 2.33) can be explained with different values of diffusion coefficient of oxygen in the U_3O_7 phase.

In the literature, one distinguishes two types of oxidation kinetics below and above 573 K approximately [20]. The diffusion coefficients of oxygen in the two phases (U_4O_9 and U_3O_7) obtained by adjustment enable to account for this change of kinetic mode. At low temperature ($T < 573$ K), the diffusion of oxygen in the U_3O_7 phase is the 'limiting step' because this one is slower than in the U_4O_9 phase. On the contrary, at high temperature ($T > 573$ K), the diffusion in the U_4O_9 phase is the 'limiting step' (Fig. 5).

The application of kinetic laws derived for unirradiated UO_2 to the case of irradiated fuel has been difficult to justify in the past, because U_3O_7 and U_4O_{9+z} predominate in the two cases. Our new model makes it possible to overcome this difficulty by modifying the stoichiometry ranges of these two phases.

As previously mentioned, for the necessity of the model, the stoichiometric ranges were fixed at [2.22–2.25] for the U_4O_9 phase and [2.32–2.33] for the U_3O_7 phase but, these limits are far from being characterized perfectly [21]. The modification of these stoichiometric ranges could involve a modification of the kinetics of weight gain which remains nevertheless low on the unirradiated UO_2 powders. On the other hand, the behaviour of spent fuel oxidation is different due to the presence of third elements such as the fission products and actinides in the matrix. Hanson [13] reports that the U_4O_9 phase is hyperstoichiometric in spent fuel with a value of the O/U atomic ratio which can reach 2.4. Taylor [22] also reminds that the distinction between the U_4O_9, U_3O_7 and UO_{2+x} phases becomes blurred at moderate to high burnups. This is principally due to the presence of fission products or actinides dissolved in the matrix which disturb the order at long distance from a crystallographic point of view. The modification of the stoichiometry ranges according to the irradiation could thus be a good manner to obtain a common kinetic law for unirradiated UO_2 and spent fuel which remains justified physically.

In addition, the burnup has only a little influence on kinetic of the transition $UO_2 \rightarrow U_4O_9$ [13,22] whereas the duration of the plateau and its value are strongly influenced [13]. Based on our model, these observations can be interpreted by considering that the diffusion coefficients of oxygen in the U_4O_9 phase ($D^O_{U_4O_9}$) should be independent of the burnup whereas $D^O_{U_3O_7}$ should be a decreasing function of the burnup (Fig. 6).

Our new grain model presented in this paper could be used to describe the oxidation kinetics of spent fuel by using the procedure of calculation suggested elsewhere [23]. The approach is based on the convolution between the model of oxidation of grains and an empirical parameter representing the propagation rate of the oxidation front into the grain boundaries.

5. Conclusions and outlooks

A model of UO_2 grain oxidation based on the step by step resolution of the oxygen diffusion equation in spherical geometry and taking into account the new experimental results [14] was confronted with the literature data. Comparisons were focused on the kinetics of oxidation obtained on UO_2 powders at various temperatures and on the determination of chemical diffusion coefficients of oxygen in the two phases (U_4O_9 and U_3O_7) formed during oxidation. By a suitable choice of diffusion coefficients ($D^O_{U_4O_9}$ and $D^O_{U_3O_7}$), it turns out that the comparison between the calculation and the experimental weight gain curves of the literature is correct during the parabolic oxidation step (in spite of uncertainties concerning grain size distribution, initial O/U atomic ratio, stoichiometry ranges). The model does not yet take into account the transition to the U_3O_8 swelling phase. The values of the diffusion coefficients obtained by fitting the oxidation model to experimental data could thus be compared with the literature data. The values are found in the panel of the 'theoretical' curves proposed by various authors (especially for U_3O_7 phase). Two apparent activation energies in the two phases (U_4O_9 and U_3O_7) could also be deduced and appears to be coherent on average with the published data ($E_a = 90$ kJ mol^{-1}).

Below 573 K, the diffusion coefficients of oxygen in the U_4O_9 phase are higher than those in U_3O_7 phase. Around 573 K, the diffusion coefficients in the two phases intersect. This result is coherent with some experimental observations which do not distinguish phase U_3O_7 from phase U_4O_9 beyond this temperature. A change of kinetic mode occurs around 573 K.

For the needs of the model; the stoichiometric ranges were fixed. But the accurate knowledge of these domains is necessary to refine the model. Consequently, some complementary experiments

allowing defining the position and the progression of the oxidation front in the grain will be carried out later.

In the future, the more elaborate grain model described in this paper will be used in the convolution procedure proposed in [23] in order to describe the oxidation of spent fuel fragments. The modelling should take into account the influence of the burnup and the variation of the stoichiometric ranges.

Acknowledgements

The authors are grateful to Electricité de France (EDF) for its financial support within the Research Program on the long term Evolution of Spent Fuel Waste Packages of the CEA (PRECCI).

References

[1] S. Aronson, R.B. Roof, J. Belle, J. Phys. Chem. 27 (1957) 137.
[2] M.J.S. Anderson, Bull. de la Soc. Chim. Française (1953) 781.
[3] M.P. Pério, Mém. Soc. Chim. de France (1953) 840.
[4] M.P. Pério, Mém. Soc. Chim. de France (1953) 256.
[5] J.S. Anderson, L.E. Roberts, E.A. Harper, The oxides of uranium. Part VII. The oxidation of uranium dioxide (1955) 3946.
[6] P.E. Blackburn, J. Weissbart, E.A. Gulbransen, J. Phys. Chem. 62 (1958) 902.
[7] R.E. DeMarco, H.A. Heller, R.C. Abbott, W. Burkhardt, Ceram. Bull. (1959) 360.
[8] H.R. Hoekstra, A. Santoro, S. Siegel, J. Inorg. Nucl. Chem. 18 (1961) 166.
[9] D.E.Y. Walker, J. Appl. Chem. 15 (1965) 128.
[10] Y. Saito, Nihon Kinzoku Gakkai-shi 39 (1975) 760.
[11] H. Ohashi, E. Noda, T. Morozumi, J. Nucl. Sci. Technol. 11 (1974) 445.
[12] R.J. McEachern, P. Taylor, J. Nucl. Mater. 254 (1998) 87.
[13] B. Hanson, PNNL-11929 report (1998).
[14] G. Rousseau, L. Desgranges, F. Charlot, N. Millot, J.C. Niepce, M. Pijolat, F. Valdivieso, G. Baldinozzi, J.F. Bérar, J. Nucl. Mater. 355 (2006) 10.
[15] Hj. Matzke, J. Nucl. Mater. 114 (1983) 121.
[16] K.W. Lay, J. Am. Ceram. Soc. 53 (1970) 369.
[17] J.H. Harding, D.G. Martin, report EUR-12402 (1989).
[18] W. Breitung, J. Nucl. Mater. 74 (1978) 10.
[19] R.J. McEachern, J. Nucl. Mater. 245 (1997) 238.
[20] Ph. Dehaudt, CEA internal report, DEC 99002 (1999).
[21] Y.S. Kim, J. Nucl. Mater. 279 (2000) 173.
[22] P. Taylor, J. Nucl. Mater. 344 (2005) 206.
[23] L. Desgranges, G. Rousseau, M.-P. Ferroud-Plattet, C. Ferry, H. Giaccalone, I. Aubrun, P. Delion, J.-M. Untrau, in: Proc. MRS, Ghent (2005).